Coccidioidomycosis seasonality in California: a longitudinal surveillance study of the climate determinants and spatiotemporal variability of seasonal dynamics, 2000–2021

Alexandra K. Heaney,[a] Simon K. Camponuri,[b] Jennifer R. Head,[c,d] Philip Collender,[e] Amanda Weaver,[b] Gail Sondermeyer Cooksey,[f] Alexander Yu,[f] Duc Vugia,[f] Seema Jain,[g] Abinash Bhattachan,[h] John Taylor,[i] and Justin V. Remais[b,*]

[a]Herbert Wertheim School of Public Health, University of California, San Diego, San Diego, CA, USA
[b]Division of Environmental Health Sciences, University of California, Berkeley, Berkeley, CA, USA
[c]Department of Epidemiology, University of Michigan, Ann Arbor, MI, USA
[d]Institute for Global Change Biology, University of Michigan, Ann Arbor, MI, USA
[e]Santa Clara County Public Health Department, San Jose, CA, USA
[f]Infectious Disease Branch, California Department of Public Health, Richmond, CA, USA
[g]San Francisco Department of Public Health, San Francisco, CA, USA
[h]Department of Geosciences, Texas Tech University, Lubbock, TX, USA
[i]Department of Plant and Microbial Biology, University of California, Berkeley, Berkeley, CA, USA

Summary

Background Coccidioidomycosis, an emerging fungal disease in the western USA, exhibits seasonal patterns that are poorly understood, including periods of strong cyclicity, aseasonal intervals, and variation in seasonal timing that have been minimally characterized, and unexplained as to their causal factors. Coccidioidomycosis incidence has increased markedly in recent years, and our limited understanding of intra- and inter-annual seasonality has hindered the identification of important drivers of disease transmission, including climate conditions. In this study, we aim to characterize coccidioidomycosis seasonality in endemic regions of California and to estimate the relationship between drought conditions and coccidioidomycosis seasonal periodicity and timing.

Methods We analysed data on all reported incident cases of coccidioidomycosis in California from 2000 to 2021 to characterize seasonal patterns in incidence, and conducted wavelet analyses to assess the dominant periodicity, power, and timing of incidence for 17 counties with consistently high incidence rates. We assessed associations between seasonality parameters and measures of drought in California using a distributed lag nonlinear modelling framework.

Findings All counties exhibited annual cyclicity in incidence (i.e., a dominant wavelet periodicity of 12 months), but there was considerable heterogeneity in seasonal strength and timing across regions and years. On average, 12-month periodicity was most pronounced in the Southern San Joaquin Valley and Central Coast. Further, the annual seasonal cycles in the Southern San Joaquin Valley and the Southern Inland regions occurred earlier than those in coastal and northern counties, yet the timing of annual cycles became more aligned among counties by the end of the study period. Drought conditions were associated with a strong attenuation of the annual seasonal cycle, and seasonal peaks became more pronounced in the 1–2 years after a drought ended.

Interpretation We conclude that drought conditions do not increase the risk of coccidioidomycosis onset uniformly across the year, but instead promote increased risk concentrated within a specific calendar period (September to December). The findings have important implications for public health preparedness, and for how future shifts in seasonal climate patterns and extreme events may impact spatial and temporal coccidioidomycosis risk.

Funding National Institutes of Health.

Keywords: Coccidioidomycosis; *Coccidioides*; Emerging infectious disease; Drought; Seasonality; Fungal infections

*Corresponding author. Division of Environmental Health Sciences, University of California, Berkeley, Berkeley, CA, 94720, USA.
   E-mail address: jvr@berkeley.edu (J.V. Remais).

Research in context

Evidence before this study

Coccidioidomycosis, a fungal respiratory disease caused by the soil-dwelling fungus *Coccidioides* spp., is emerging as a significant concern in the southwestern US, with reported cases doubling across the country and tripling in California since 2014—where *Coccidioides immitis* is the dominant species. We searched for studies published in English up to September 14, 2023, with the terms "coccidioidomycosis AND California AND season AND (climate OR drought OR precipitation)" in PubMed and identified 18 results published between 1964 and 2023. Although some previous studies note an unimodal seasonal pattern with peaks during the fall season in California, the seasonality of coccidioidomycosis in California has not been fully characterized concerning seasonal onset, periodicity, and regional and annual variation. Several studies point to wet-dry climate cycles as key drivers of transmission dynamics, with precipitation facilitating pathogen growth and dry conditions supporting spore formation and dispersal. Some work shows that coccidioidomycosis incidence peaks at the end of dry seasons in Arizona and California, especially following anomalously wet winters and dry summers. One study published in 2022 indicates that drought conditions are associated with low incidence in California in the short term but amplify incidence in subsequent years. However, the impact of severe multi-year droughts on the seasonal cycles of coccidioidomycosis has not been assessed. Unravelling these complexities is essential for effective public health planning and risk assessment, particularly in the context of global climate change.

Added value of this study

In this study, we provide a comprehensive characterization of coccidioidomycosis seasonal dynamics and their climate determinants in California. From 2000 to 2021, we observed that monthly coccidioidomycosis incidence across California counties peaked between September and November, at the end of the dry season, and was lowest from April to June, at the end of the wet season. Yet, we found significant heterogeneity in the strength and timing of seasonality across counties and transmission years, including heterogeneity in whether a seasonal amplification of incidence occurred. We demonstrate that a significant amount of the variability in seasonal patterns can be explained by cyclical climate conditions. Seasonal fall peaks in incidence are more pronounced following a wetter-than-average wet season and a drier-than-average dry season. There is growing evidence that wet conditions followed by dry conditions promote

coccidioidomycosis risk. However, rather than increasing risk of coccidioidomycosis uniformly across the year, we show that these conditions increase risk specifically during the fall season. Our results also demonstrate that shifts in local climate from drought conditions to wet conditions lead to more pronounced seasonal peaks in coccidioidomycosis incidence.

Implications of all the available evidence

Our findings indicate that peak incidence occurs between September and November. Accounting for estimated incubation periods and diagnosis delays, our results suggest that the period of highest risk of *C. immitis* exposure in California typically occurs between July and September and the lowest risk of exposure occurs from February to April. However, the timing and strength of seasons differed across regions of the state. This information can guide region-specific timing of public health messaging, advising individuals to avoid dusty environments and dust-generating activities during these months and encouraging the use of measures to mitigate dust exposure, such as soil wetting, N95 masks, and air filtration systems. Furthermore, communication regarding periods of high risk can inform medical practitioners about when to be particularly vigilant for new cases. This is especially useful because prompt diagnosis and case management can improve disease outcomes.

Our findings can aid the creation of accurate and timely early warning systems and forecast models in a changing climate. California's drought risk is expected to rise due to global climate change, leading to more frequent droughts and the likelihood of prolonged megadroughts in the coming decades. Our results and other existing work suggest that the increase in drought conditions will impact both the incidence and seasonal patterns of coccidioidomycosis. Specifically, future droughts may suppress both annual incidence rates and seasonal peaks during the drought period, leading to low levels of cases sustained throughout the year. When the drought ends, there will be elevated cases concentrated during the fall season that follows. Moreover, the effects of drought are amplified when followed by anomalously high rainfall, and this extreme dry-wet cycling is expected to occur more frequently under climate change. This, coupled with the geographic expansion of coccidioidomycosis, will likely elevate disease risk for California's population. Further analyses should consider how the associations revealed in this study can be used to generate accurate disease forecasts and guide mitigation activities.

Introduction

Many infectious diseases display seasonality, commonly observed as a periodic rise in incidence during specific seasons or calendar periods. Examination of seasonal disease trends can support the identification and understanding of mechanisms underlying disease dynamics, including those related to climate and environmental forcings of pathogen survival or infectivity

and host ecology. For example, influenza generally displays peaks in incidence during cold winter months in the Northern Hemisphere during non-pandemic periods, thought to be driven in part by increased virus survival in colder and drier environmental matrices.[1–3] Characterizing the timing and strength of seasonal infectious disease surges also has clear public health benefits. These include aiding disease prediction, prevention, and mitigation, enabling the development of more accurate surveillance systems, and anticipating and planning for future disease risks in the context of global climate change.[4]

Coccidioidomycosis is an emerging infectious disease in the southwestern U.S. caused by inhalation of aerosolized spores of the *Coccidioides* genera, primarily *C. immitis* and *C. posadasii*.[5,6] Since 2014, annual reported cases of coccidioidomycosis have nearly doubled across the United States[7] and more than tripled in California, where *C. immitis* is the dominant species.[7] Furthermore, the geographic range of coccidioidomycosis is expanding, with the largest incidence increases in California reported outside of historically highly endemic regions.[8] Some limited prior research in California suggests that coccidioidomycosis incidence has an unimodal seasonal pattern with peaks most often observed in October.[9] However, variations in seasonal dynamics across regions and the role of changing climate and other factors in determining these patterns remain unclear.

The importance of climate as a seasonal driver for many infectious diseases is often explained by mechanisms that relate to the environmental biology of pathogens and/or the ecology of hosts and vectors.[4,10] For coccidioidomycosis, epidemiological evidence suggests that wet followed by dry climate conditions may be important drivers of seasonal transmission dynamics.[6,11–16] *Coccidioides* spp. grow saprotrophically as filamentous mycelia with alternating cells that differentiate and autolyze to form heat-tolerant, infectious spores termed 'arthroconidia'.[6] Prevailing mechanistic hypotheses suggest that total seasonal precipitation and resultant soil moisture facilitate the growth and sporulation of *Coccidioides* spp.,[11,17] while hot and dry conditions support the formation of arthroconidia and enable the dispersal of spores from soil during episodic wind erosion or soil disturbance.[9,14–16,18,19] Indeed, seasonal coccidioidomycosis incidence peaks at the end of dry seasons in Arizona and California,[9,14] especially following anomalously wet winters and dry summers.[15] Recent research using highly spatiotemporally resolved incidence data in California found that drought conditions are associated with low coccidioidomycosis incidence in the short term, but amplify incidence in subsequent years.[15] However, it remains unclear how disruptions to seasonal wet-dry climate cycles—such as those caused by severe multi-year droughts—affect seasonal cycles of coccidioidomycosis.

Here, we characterize coccidioidomycosis seasonality across endemic counties in California and estimate the relationship between climatic conditions, drought, and coccidioidomycosis seasonal periodicity and timing. We analyze surveillance data in California from 2000 to 2021 to characterize the periodicity and timing of coccidioidomycosis seasonality across California counties and use high-resolution temperature and precipitation anomaly data to investigate the impact of drought conditions on county-level seasonality across the study period. We discuss the implications of our findings for the prediction of case surges, and promotion of individual- and community-level protective measures. A better understanding of seasonal trends can elucidate relationships between inter- and intra-annual climate variability (i.e., temperature and precipitation anomalies) and disease dynamics, and the results are discussed as to their implications for how future shifts in seasonal climate patterns and extreme events may impact spatial and temporal coccidioidomycosis risk.

Methods

Epidemiological data

We conducted a longitudinal surveillance study leveraging information on all confirmed coccidioidomycosis cases that occurred among California residents between April 1, 2000, and April 1, 2021, which we obtained from the California Department of Public Health (CDPH) coccidioidomycosis surveillance system. All healthcare providers and laboratories in California are required to report diagnosed cases of coccidioidomycosis to local health departments and CDPH.[20] Detailed descriptions of case data processing can be found in the Supplementary Material. Briefly, we computed monthly case totals per county from georeferenced incident cases. We geocoded patient addresses (available for 95% of cases) using ArcGIS to determine their county of residence. Case onset dates were available for 24% of cases; otherwise, we used the earliest clinical or laboratory date as an estimated onset date to account for reporting delays. The study region encompassed 17 counties that had an annual mean incidence rate exceeding 10 cases per 100,000 population, a threshold used to ensure that each spatial unit had sufficient data to support wavelet transform analyses. Counties were grouped into five CDPH-defined regions[8]: Northern San Joaquin Valley, Southern San Joaquin Valley, Central Coast, Southern Inland, Southern Coast. County-level population estimates were obtained from the California Department of Finance.[21,22] All data were de-identified prior to analysis. While enhanced surveillance studies have identified significant delays between symptom onset and diagnosis with coccidioidomycosis (on average, about 2–5 weeks),[23,24] we did not explicitly correct for

reporting delays in our data due to the large variability and uncertainty of reporting delays among patients and the lack of specific data on reporting delays in California. The study received approval from the Committee for Protection of Human Subjects of the California Health and Human Services Agency (protocol no. 17-05-2993). Approval by the University of California, Berkeley, was provided by reliance on the California State approval. Upon human subjects' review, the study was granted a waiver of informed consent consistent with 45 CFR 46.116(f).

Meteorological data and standardized precipitation-evapotranspiration index (SPEI)

We obtained daily gridded total precipitation and maximum and minimum temperature from the Daily Observational Hydrometeorological data set produced by the Cooperative Institute for Research in Environmental Sciences (CIRES) (6-km resolution; 1950–1980)[25] and from the Parameter-elevation Regression on Independent Slopes Model (PRISM) Climate Group (4-km resolution, 1981–2021).[26] We used these data to compute total monthly rainfall and average monthly maximum and minimum temperature for each county. To quantify drought severity, we calculated a county-level standardized precipitation-evapotranspiration index (SPEI) using total monthly precipitation and maximum and minimum monthly temperature measurements from 1950 to 2021. SPEI is a multi-scalar index of climatic water balance, incorporating both water input via precipitation as well as evaporative demand, measured by potential evapotranspiration (PET). SPEI values represent the number of standard deviations by which the climatic water balance deviates either below (drier) or above (wetter) the long-term average. For each county, we calculated monthly PET values[27] and monthly SPEI following the Vicente Serrano et al. methodology.[28] SPEI can be calculated on a range of time scales, and we specifically calculated 3-month (shorter time-scale) and 12-month (longer timescale) SPEI. We defined periods of drought using SPEI cutoffs based on the US Drought Monitor (USDM); SPEI < −0.5 were classified as drought conditions and lower SPEI values indicated more severe drought (e.g., SPEI ≤ −2 = exceptional drought [USDM D4]).[29]

Characterizing coccidioidomycosis seasonality using wavelet transformation

We conducted a wavelet analysis with the Morlet function as the wavelet base using the WaveletComp (ver. 1.1) package in R (ver. 4.2.1).[30] Broadly, wavelet analysis is a mathematical technique used to decompose a signal into components that vary over different scales or frequencies. Wavelet analysis applied to infectious disease time series data decomposes the incidence time series into components that represent the data's behaviour at different time scales. This method is particularly suited to analyzing disease cyclicity (i.e., seasonality) because it can identify the relative strength and timing of dominant cycles in incidence.

Monthly county-level coccidioidomycosis incidence rates were normalized to have a mean of zero and a unit variance (Supplementary Figures S1–S3) within each county year and then detrended using a loess smoothing function. This procedure removes annual, interannual, and spatial heterogeneity in incidence from the time series, i.e., it generates a time series with comparable amplitudes across all transmission years (defined as March–February) and counties. Doing so ensures that wavelet transformation reflects the periodicity of the time series and not the variability in incidence across counties or years. Detrending and normalizing the incidence data allows isolation and comparison of seasonal signals between counties and years. As such, the results are solely related to the relative strength of seasonal signals and do not address any multiyear trends in incidence.

Wavelet transformations were performed on each normalized and detrended county time series. Each wavelet transformation generated (1) local wavelet power spectrums, which indicate time-frequency distribution and predominant signal components across the study period and (2) corresponding phase angles, which indicate the relative timing of different signal components. The power associated with the wavelet coefficients indicates the strength or intensity of the signal at various scales and times. Here, we are most interested in the 12-month scale, which represents a cycle in which disease incidence peaks regularly once per year. A higher power value at a 12-month scale would suggest a stronger seasonal component in the data, while a lower power value would indicate a weaker seasonal component to the data. Periods of statistically significant power (alpha defined as 0.05) were determined using a bootstrapping method whereby distributions of power spectra were produced using 2000 different time series that represent randomly shuffled versions of the original incidence time series. Power spectra for each county are reported in Supplementary Figures S5–S21.

Wavelet transforms for each county indicated that the annual component was dominant (i.e., the highest power estimates centered around signals with 12-month periodicity) (Supplementary Figure S24). To further explore the annual seasonality (i.e., 12-month periodicity) of incidence between counties and time periods, we extracted monthly power and phase angle estimates for the annual signal component. We calculated average power across counties and transmission years to determine how the annual signal strength varied across space and time. We used the phase angles to analyze the synchrony of annual signals across counties and years. To determine the synchrony of

more than 2 different time series, we calculated the mean absolute phase difference, defined as the absolute value of the mean of all combinatorial pairwise phase differences between time series in each month. See more details about power interpretation and phase angle calculations in the Supplementary Methods.

Estimating the impact of drought on annual wavelet power

We used distributed lag nonlinear regression models (DLNMs) to flexibly estimate the association between drought conditions (SPEI) and coccidioidomycosis seasonality. For each county and transmission year (March–February), we calculated 12-month (annual) SPEI as well as 3-month (seasonal) SPEI for spring (March–May), summer (June–August), fall (September–November), and winter (December–February). We used DLNMs to estimate the associations between 12-month (annual) SPEI lagged 0–6 years and 3-month (seasonal) SPEI lagged 0–2 years and average wavelet power in a transmission year. Average wavelet power was calculated as the mean monthly power at a 12-month periodicity across each transmission year and for each county. The magnitude of average annual power here serves as an indicator of the strength and consistency of 12-month seasonal signals in disease incidence in each year. Both annual and seasonal models took the following form:

$$P_{i,t} = \beta_0 + f(SPEI_t, l, \theta) + \beta_i County_i + s(year) + \varepsilon_{i,t}$$

where $P_{i,t}$ represents the average power in county i in year t; β_0 is the intercept term; $f(SPEI_t, l, \theta)$ is a cross-basis function $\int_{l=l_0}^{L} SPEI_{t-l} * s(l, \theta)$ in which $SPEI_{t-l}$ indicates a linear exposure-response relationship between annual power and SPEI at each lag l; $s(l, \theta)$ represents a natural cubic spline of the lag-response relationship between SPEI and annual power; and θ is a vector of coefficients for the spline $s(l, \theta)$.[31] To determine the knot locations for the natural cubic spline, we systematically varied the number and location of the knots placed along the lag dimension and selected the model that produced the lowest Akaike information criterion. We conducted sensitivity analyses with various knot specifications and found similar results regardless of knot placement and spline specification (Supplementary Figures S22 and S23). Both models included a fixed effect for county to adjust for differential case reporting, spatial clustering, and other spatial factors not explained by SPEI, and a natural cubic spline on year to adjust for long-term temporal trends across the study period.

We further examined how drought duration influenced annual wavelet power *after the drought* using generalized additive models. We assigned a month as a "drought month" if the 12-month SPEI for that month was below –0.5 (D0-D4), following the methods specified by

the US Drought Monitor.[29] Drought duration was defined as the number of consecutive months in which the 12-month SPEI was below –0.5. This model took the form:

$$P_{i,t+1} = \beta_0 + s(duration_{i,t}) + \beta_i County_i + s(year_{t+1}) + \varepsilon_{i,t}$$

where $s(duration_{i,t})$ indicates a natural cubic spline on the duration of drought that ends in year t in county i, and $P_{i,t+1}$ indicates the annual average power in county i in the year following the end of the drought (year $t+1$); β_0 represents the intercept term. Models included a term for county and a natural cubic spline on year to adjust for unmeasured spatial and temporal confounders. To examine the sensitivity of our findings to various drought definitions, we conducted this analysis for a drought definition of SPEI < –0.8 (D1-D4) and SPEI <0 (any anomalously dry periods).[29]

Role of the funding source

The funding source did not have any role in study design, data collection, data analysis, interpretation, or writing of the report.

Results

Seasonal patterns in coccidioidomycosis incidence

Over the study period from March 2000 to February 2021, there were 89,281 reported coccidioidomycosis cases across 17 counties, of which 62.2% were male and 37.8% were female. The annual incidence across counties in 2018 (32.08 cases per 100,000 population) was 12 times higher than in 2000 (2.58 cases per 100,000 population), with the largest proportional increases in annual incidence observed in Monterey (8248% increase), San Joaquin (4369% increase), Fresno (4920% increase), San Luis Obispo (4222% increase) and Ventura (2612% increase) counties. The highest average annual incidence rates were observed in Kern County (199.0 cases per 100,000 population) followed by Kings (80.3 cases per 100,000 population), San Luis Obispo (53.6 cases per 100,000 population), and Tulare counties (50.3 cases per 100,000 population) (Fig. 1a). Across all years and counties, the months with the highest proportion of annual cases were September, October, and November (Fig. 1c and Supplementary Figure S4). However, the monthly distribution of annual cases varied greatly between counties and years (Fig. 1b and c). Some years, such as 2010 and 2016 (Fig. 1b), had stronger seasonal patterns (i.e., cases were more concentrated during the fall months) and some years, such as 2007 and 2014, did not exhibit strong seasonal patterns (i.e., cases were more evenly distributed across the year). Average seasonal patterns of incidence, precipitation, and temperature across all included counties are shown in Supplementary Figure S4.
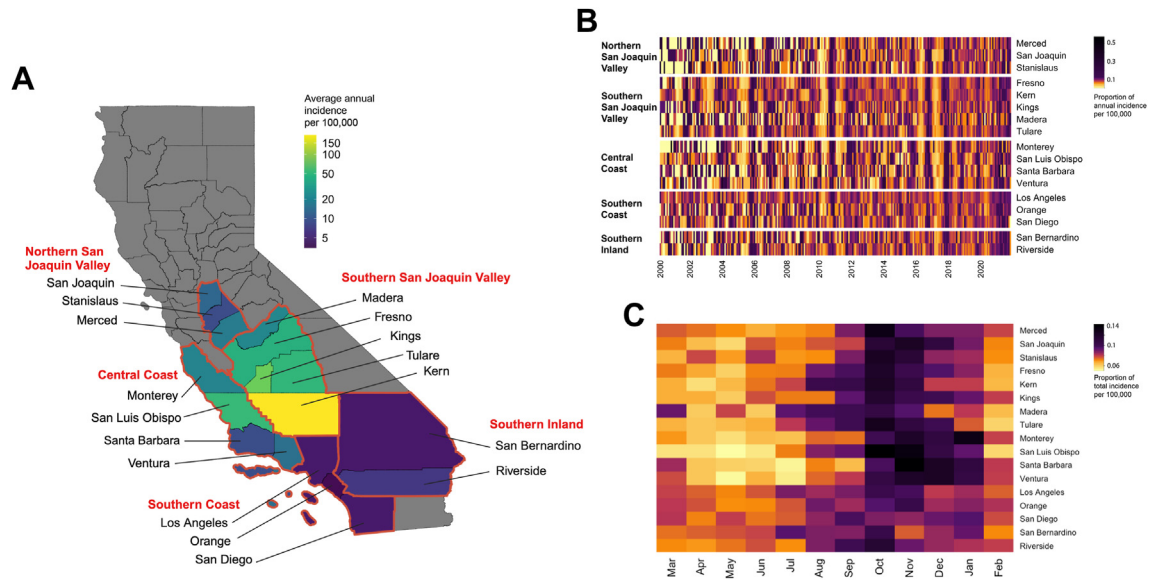
Fig. 1: (A) Mean annual incidence of coccidioidomycosis between the years 2000 and 2021. Counties included in the analyses are outlined and labeled in black. Regions are outlined and labeled in red. (B) Heat map of the proportion of coccidioidomycosis incidence in each month across all 17 included California counties from 2000 to 2021. Colors represent the proportion of annual cases—defined by transmission year (March–February)—that occurred in each month. Counties are grouped by the five California Department of Public Health-defined regions with consistently high incidence of Northern San Joaquin Valley, Central Coast, Southern San Joaquin Valley, Southern Coast, and Southern Inland, and counties within groups are ordered by decreasing latitude of centroids. (C) Heat map of the proportion of coccidioidomycosis incidence in each month across all included California counties from 2000 to 2021. Colors represent the monthly proportion of total incidence across all years, and counties are grouped by region and county centroids as in (b).

Annual periodicity characterized by wavelet transforms

We observed significant 12-month periodicity across all counties, indicating sharp seasonal increases in incidence, on average, once every 12 months (Supplementary Figure S24). Accordingly, from here forward, we use "power" to indicate the power associated with the wavelet component with a 12-month periodicity, which indicates the strength and consistency of seasonal cycles in disease incidence. There was considerable heterogeneity in the power spectra across counties and years (Fig. 2a, Supplementary Figure S5-S21, and S25). While all counties except Madera demonstrated statistically significant annual seasonality averaged across the study period (Supplementary Figure S24), no county showed statistically significant annual periodicity in every study year (Fig. 2b). Kern County had the most consistent detection of annual periodicity from 2000 to 2021, with statistically significant power in 85% of the study period (Fig. 2b). In contrast, San Bernardino and Madera Counties did not exhibit statistically significant annual periodicity over most of the study period (Fig. 2b).

Some periods displayed more significant annual periodicity (i.e., statistically significant wavelet components at 12-month periodicity) across counties than others (Fig. 2a and b). From 2010–2012 and 2016–2018,

12 (71%) and 16 (94%) of the 17 counties, respectively, displayed statistically significant annual periodicity. In contrast, from 2012–2014 and 2019–2022, only 3 (18%) and 2 (12%), respectively, of the 17 counties exhibited significant annual periodicity (Fig. 2a and b). Temporal trends in county-level average power across transmission years also confirmed these patterns. The highest average power estimates across counties occurred in the 2010, 2016–2018 transmission years and the lowest average power estimates occurred in the transmission years in the ranges 2012–2014 and 2019–2021 (Fig. 2c).

Geographically, the average power in counties in the Southern San Joaquin Valley (0.38) and Central Coast (0.35) was higher than in the Northern San Joaquin Valley (0.19), Southern Coast (0.18), and Southern Inland counties (0.24) (Fig. 3). Kern County had the highest median power (0.66), while Stanislaus County had the lowest median power (0.12) (Fig. 3a).

Timing of annual seasonal patterns characterized by wavelet transforms

By analyzing phase differences, we found that, on average, the annual seasonal cycle in Southern San Joaquin Valley and Southern Inland occurred earlier than that of those in Northern San Joaquin Valley, Central Coast, and Southern Coast (Fig. 4). The season began earliest (i.e., highest positive phase differences) in Kern, Fresno, and Tulare
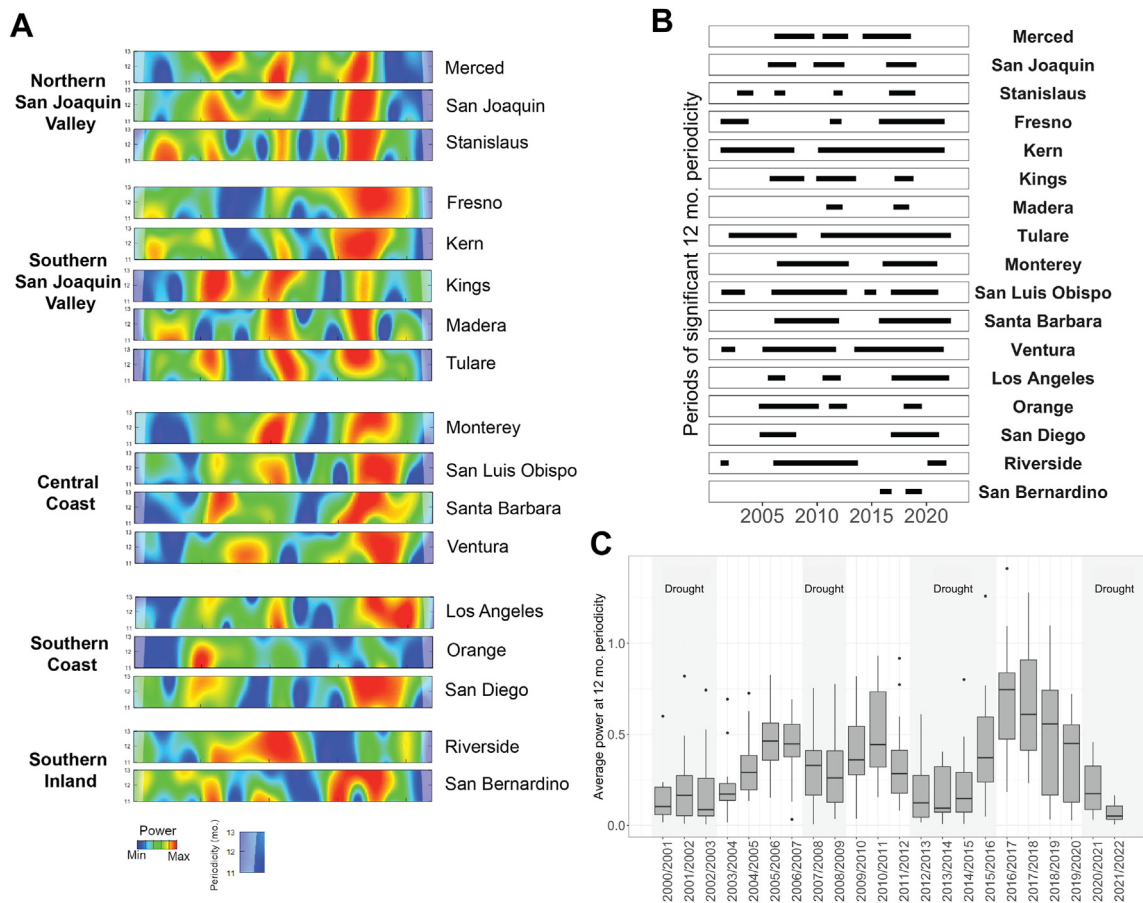
Fig. 2: (**A**) The power spectrum from wavelet analyses for each county and periodicities 11–13 months (y-axis) from 2000 to 2021 (x-axis). The power color scale is a relative scale spanning the maximum and minimum power estimates for each county. Supplementary Figures S5–S21 show the numerical power estimates for each county. (**B**) Periods of statistically significant (p < 0.05) 12-month periodicity for each county from 2000 to 2021 shown as black lines. (**C**) Boxplot of county-level average power across transmission years (defined as March–February). Light grey shading shows periods of moderate to severe drought in California as defined by the U.S. Drought Monitor (2000–2002; 2007–2009; 2012–2015; 2020–2021).[29]

Counties, and the latest (i.e., lowest negative phase differences) in Merced, Monterey, and Santa Barbara Counties (Fig. 4 and Supplementary Figure S26).

Absolute mean phase differences were between 0 and 3 months for all transmission years (Supplementary Figure S27), indicating that seasonal peaks were all within 3 months of each other. However, there was heterogeneity in mean phase differences across transmission years (Supplementary Figures S27 and S28). County-level seasonal timings were most synchronous (e.g., absolute mean phase differences were lowest) during the 2016–2019 transmission years, while seasonal timings were least synchronous (i.e., absolute mean phase differences were highest) during the 2012 and 2013 transmission years (Supplementary Figures S27 and S28). A nonlinear GAM model revealed a negative trend in mean absolute phase difference over the study period, indicating that county-level annual seasonal timing became increasingly aligned over the study period (Supplementary Figure S29).

### Association between SPEI and average annual power at 12-month periodicity

Transmission years during periods of severe drought conditions—as defined by the US Drought Monitor[29]—appeared to have lower seasonal wavelet power than transmission years without severe drought conditions (Fig. 2c). Annual SPEI was negatively associated with annual power in the 1–5 years prior to the transmission year, meaning prolonged anomalously dry conditions in the previous 1–5 years were associated with higher power during the transmission year (Fig. 5a and Supplementary Figure S22). We found a significant positive association between annual power and seasonal SPEI in the preceding winter, concurrent spring, and concurrent winter seasons (Fig. 5b and Supplementary
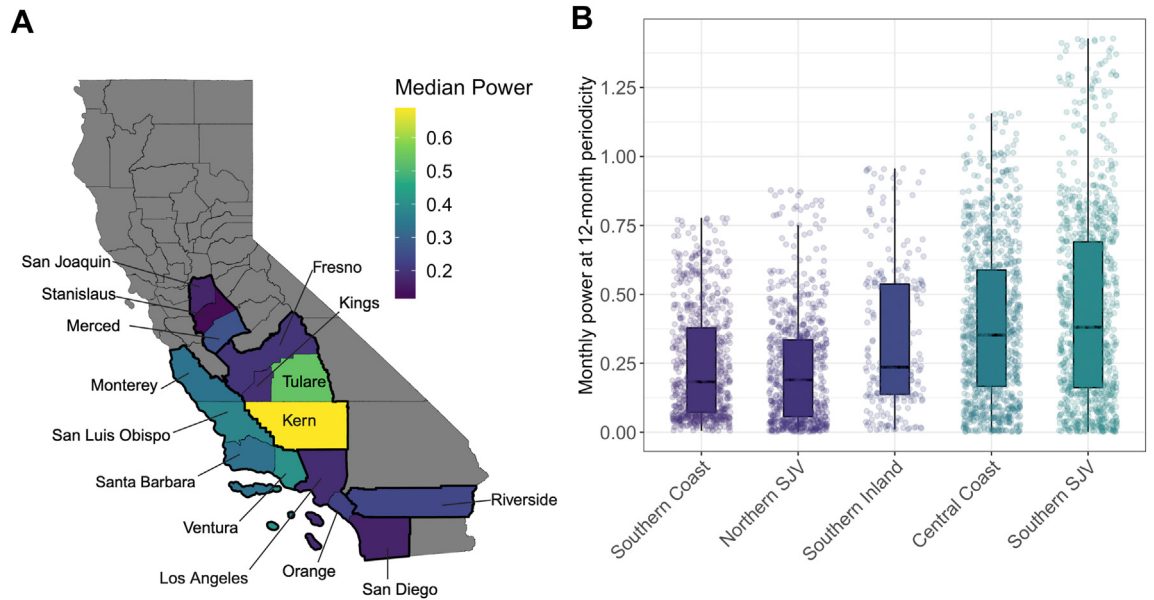
Fig. 3: (**A**) Map of median power at 12-month periodicity for each county in the study region from 2000 to 2021. CDPH-defined endemic regions are outlined with black lines. (**B**) Boxplot of monthly power at 12-month periodicity across all counties and years within each of the five CDPH-defined[8] endemic regions (x-axis). SJV = San Joaquin Valley.

Figure S23). In other words, anomalously wet conditions in the spring and winter seasons were associated with higher annual power in the same year, as were anomalously wet conditions during the prior winter. However, SPEI in the concurrent fall and summer seasons was negatively associated with annual power, indicating that anomalously dry conditions in these calendar periods were associated with more pronounced seasonal peaks (Fig. 5b). San Bernardino and Madera counties were excluded from these analyses because of
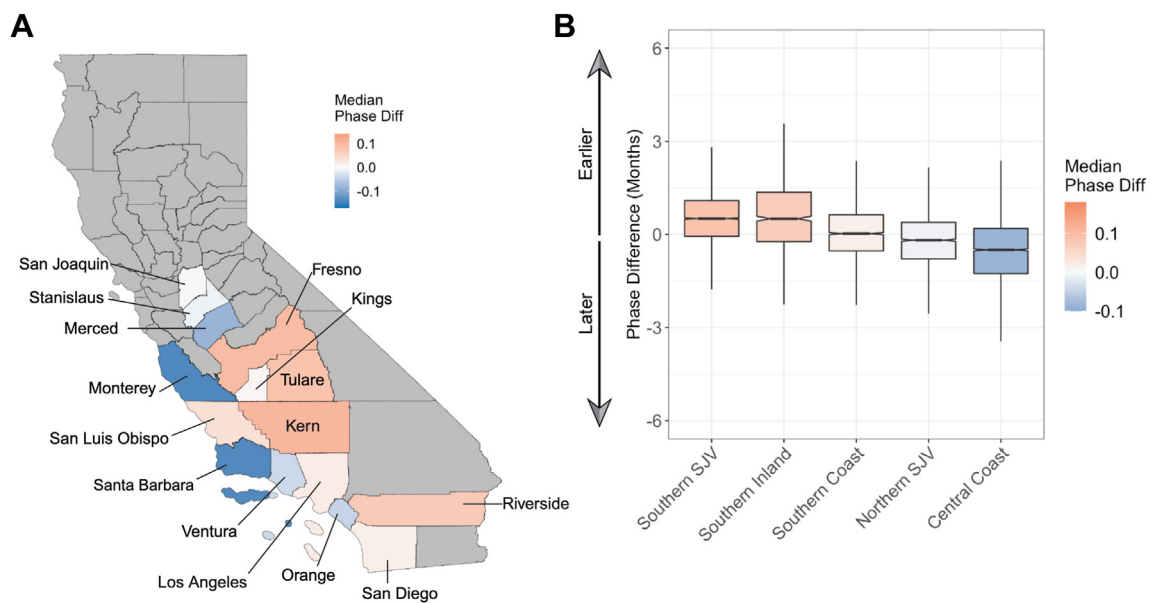
Fig. 4: (**A**) Map of the median monthly phase difference of each county from all other counties from 2000 to 2021. Orange colors represent earlier seasonal coccidioidomycosis cycles and blue represents later seasonal cycles. (**B**) Boxplots of the difference in monthly phase at 12-month periodicity between each county and all other counties from 2000 to 2021. Regions are ordered by decreasing median phase difference.
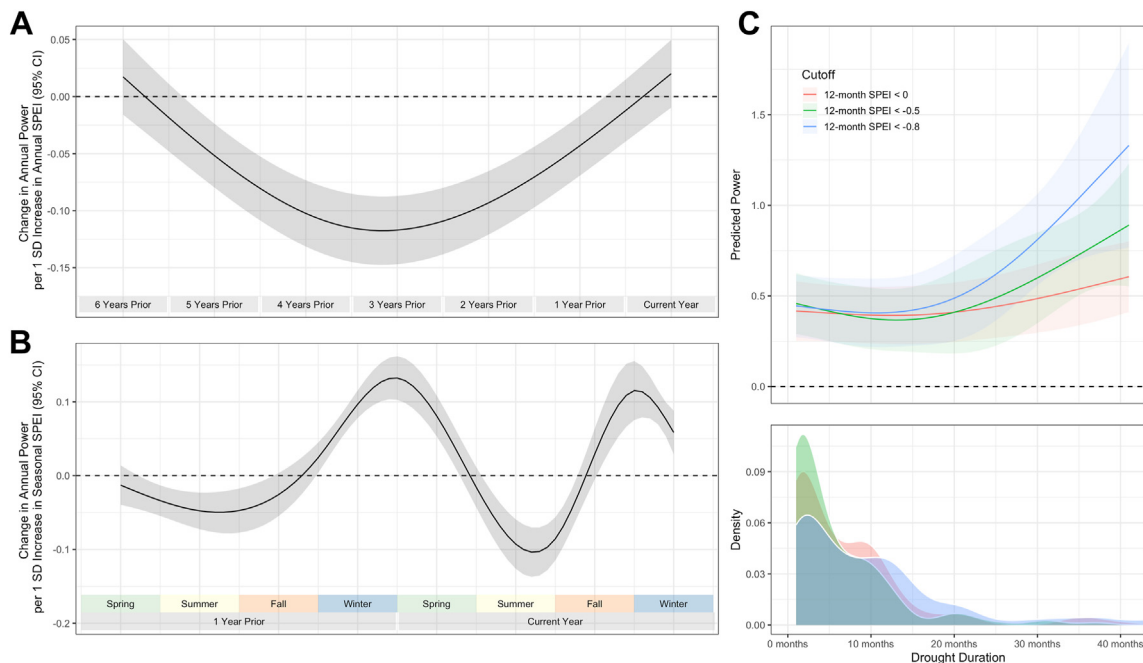
Fig. 5: Results of distributed lag nonlinear model estimating the association between annual wavelet power and (**A**) shorter-term seasonal (3-month) SPEI and (**B**) longer-term annual (12-month) SPEI. Estimates at each lag represent the increase in annual wavelet power per 1 standard deviation (SD) increase in seasonal SPEI, with the 95% confidence interval represented by the grey shading. The dashed line indicates the null hypothesis that there is no effect of SPEI on annual power. (**C**) Model predictions of annual wavelet power following droughts of various lengths were obtained from a generalized additive model, with the density of observations for drought durations shown beneath. The colored lines indicate different drought definitions (red = SPEI <0; green = SPEI < –0.5; blue = SPEI < –0.8).

their highly inconsistent annual seasonality (i.e., power at 12-month periodicity) across the study period.

Using GAMs, we found a positive association between drought duration and annual power in the transmission year immediately after the drought, but only when the drought (across all severities D0-D4) lasted longer than 15 months (Fig. 5c). The shape of the estimated exposure-response relationship differed slightly based on the definition of drought use, with a stronger positive association found when using more extreme definitions of drought (Fig. 5c).

Discussion

In this study, we provide a comprehensive characterization of coccidioidomycosis seasonal dynamics and their climate determinants in California. Over the study period from 2000 to 2021, we observed that monthly coccidioidomycosis incidence across California counties peaked between September and November, at the end of the dry season, and was lowest from April to June, at the end of the wet season. An enhanced surveillance study in Arizona found that the incubation period for coccidioidomycosis is about 7–12 days and the time from symptom onset to diagnosis is likely around 2–5 weeks.[24] Together with these estimates, our results

suggest that peak exposures to *C. immitis* are likely occurring on average between July and September and lowest exposures are likely occurring between February to April. Yet, we found significant heterogeneity in the presence, strength, and timing of seasonality across counties and transmission years. Notably, no county demonstrated significant annual seasonality in every year of the study period, but certain counties (e.g., Kern, Tulare) showed more consistent annual seasonality than others (e.g., San Bernardino, Madera). Annual seasonality was strongest on average in the Southern San Joaquin Valley and Central Coast regions. We found that while the earliest seasons, on average, occurred in the Southern San Joaquin Valley (generally hotter and drier climate) and the latest occurred in the Central Coast (generally cooler and wetter climate), the seasonal timing becomes more synchronous among counties over the course of the study period.

California has a distinct dry season (April–October) and wet season (November–March) each year, and our results show that coccidioidomycosis seasonal peaks occur most often at the end of the dry season. Anomalously wet conditions in the prior wet season as well as anomalously dry conditions during the concurrent dry season are associated with more pronounced seasonal peaks in incidence (Fig. 5b). These results are in

agreement with previous research findings that wet conditions followed by dry conditions may promote *C. immitis* growth and dispersion, resulting in increased coccidioidomycosis risk.[6,11–16] In the saprobic stage of *C. immitis* life cycle, soil moisture is required to initiate the germination of spores into mycelia, and mycelia respond to prolonged dry periods by producing a resistant form called arthroconidia, which are able to survive in dry environments and light enough to disperse, causing infection when inhaled.[11–13] Epidemiological and experimental work has shown that wet-dry cycles can promote pathogen abundance in soils and the ability of the pathogen to disperse concurrent with fugitive dust emissions.[9,14,16,18,32] Anomalously wet conditions at the end of the transmission year are associated with more pronounced seasonal peaks. This is likely because wet conditions suppress dust emissions by promoting vegetation growth and increase deposition of airborne *Coccidioides* arthroconidia, thereby driving down coccidioidomycosis incidence at the end of the season.

Regional heterogeneity in climate may contribute to the spatial heterogeneity observed in coccidioidomycosis seasonal strength and timing. The earliest seasons, on average, occurred in the Southern San Joaquin Valley and the latest seasons occurred in the Central Coast region. These findings align with work showing that coastal counties had a higher proportion of coccidioidomycosis cases in the winter, while the lower San Joaquin Valley counties had a higher proportion of cases in the fall.[9] The Southern Inland region demonstrates an earlier coccidioidomycosis season than the Central Coast region, which may be due to warmer temperatures earlier in the year in the Southern Inland (Supplementary Figure S30), potentially enabling the lysis of mycelia and dispersion of arthroconidia via dust emissions earlier in the year. Regional variability in soil composition may also play a role in the heterogeneity of seasonal strength and timing between regions. Sandy, alkaline and high salinity soils are thought to be most favourable for *C. immitis* proliferation,[11] yet soil composition varies widely across endemic California regions.[33] Differences in soil texture, porosity, density, and temperature may influence the life cycle of *Coccidioides*, and alter the impacts of climate on fungal growth and dispersion. Future research should examine how changes in seasonal patterns of temperature and precipitation (e.g., delayed and/or extreme wet season) may manifest in spatiotemporal differences in coccidioidomycosis seasonal dynamics. Despite these differences, we showed an increased synchrony of seasonal timing among counties, which may be explained by improved surveillance and reporting of cases over time, particularly in regions with emerging diseases.

Our characterization of coccidioidomycosis seasonality provides key insights into cyclical climate drivers of disease transmission. Prior work found that winter rainfall following anomalously dry conditions increased coccidioidomycosis incidence in California, and estimated that the 2007–2009 and 2012–2015 droughts resulted in decreased cases during the droughts but increased cases following the droughts.[15] Our results build upon these findings, demonstrating that drought conditions suppress coccidioidomycosis seasonality, but that transitions from drought to wet conditions lead to more pronounced seasonal peaks in California. In other words, drought followed by wet conditions does not increase the risk of coccidioidomycosis onset uniformly across the year but instead promotes risk concentrated within a specific calendar period. We expand our understanding further by showing that longer droughts have stronger impacts on coccidioidomycosis cyclicity.

Several mechanisms may explain the observed associations between drought, coccidioidomycosis risk, and seasonal dynamics. Firstly, prolonged drought conditions may offer *C. immitis* a competitive advantage by reducing microbial competitors, allowing *C. immitis* to expand into new niches once favourable conditions return.[9,32,34] Drought conditions reduce microbial activity in the soil.[35] Indeed, drought has been shown to increase the ratio of fungi to bacteria, attributable in part to fungi being better able to transfer moisture from water-filled micropores in the soil.[35] Then when moisture and nutrients return to the soil following a drought,[36] *C. immitis* can proliferate without competing against other microbes. This would increase fungal population abundance in the soil and, following spore dispersal, possibly lead to higher coccidioidomycosis incidence.

Alternatively, drought may impact *C. immitis'* mammalian hosts. Rodents have been consistently associated with *C. immitis* and *C. posadasii*, through detection in rodent burrows,[37–39] rodent lungs,[40] and in previously *Coccidioides*-negative soils following the burial of experimentally infected mice.[41] Droughts can cause rodent population declines,[42] and the resulting decomposition may supply nutrients and moisture for the *C. immitis* population to survive and expand. These potential mechanistic effects would likely intensify due to longer and more severe drought conditions. Lastly, droughts can enhance dust emissions via decreases in vegetation leading to increased wind erosion,[43–45] which may enhance exposure to airborne *C. immitis*.

With rising coccidioidomycosis incidence, understanding seasonal trends in incidence across endemic counties can guide prevention and control efforts. Given estimates of the incubation period and time from onset to diagnosis,[24] our findings suggest that peak *C. immitis* exposures typically occur between July and September but that timing is region and county-specific. This information can help tailor public health messaging, for instance about when to avoid particularly dusty environments and dust-generating activities and, when dust exposure is not avoidable, when to use dust suppression techniques, such as wetting soil before disturbing, or

the use of N95 masks to prevent inhalation of *C. immitis* spores.[46–48] Healthcare professionals can also be better prepared during these peak months. Travellers to high-incidence areas, especially vulnerable individuals (e.g., immunocompromised, pregnant women), can benefit from risk awareness. It is important to note, though, that while disease risk is higher during the summer and fall months in California, cases still occur year-round and testing for coccidioidomycosis should therefore not be season-dependent among patients presenting with relevant symptoms. Furthermore, an improved understanding of seasonal dynamics can enhance early warning systems and forecasting models.[4]

Our work has several limitations that should be considered when interpreting the results. We rely on coccidioidomycosis case data representing human infection rates in California based on residential addresses and estimated disease onset dates. However, this data may not precisely reflect the environmental presence, concentration, or distribution of *C. immitis*. This limitation hinders our ability to elucidate the mechanisms of spore aerosolization and transport. Furthermore, assigning incident cases to months based on the estimated disease onset date might not always align with the true exposure or symptom onset dates due to diagnosis delays, potentially introducing biases in estimating seasonal timing. Aggregating cases at the county level may obscure sub-county variations, even as county-level information may indeed be most useful for local public health decision-making. Patients may also have been exposed outside their residence counties; investigating whether weak seasonal trends in specific counties are due to true local acquisition or travel-related exposure requires further research. Additionally, while this study focuses on drought-related cyclical patterns, future work should also consider other seasonal factors such as rodent abundance and human interactions with soils (e.g., via crop cycles or construction activities).

Lastly, our results are specific to the transmission dynamics of *C. immitis* in California and should not be generalized to other endemic regions where *C. posadasii* dominates. Phenotypical disparities between *C. immitis* and *C. posadasii*, particularly in thermotolerance—where *C. immitis* thrives at 28 °C compared to *C. posadasii* at 37 °C[49]—may drive different seasonal disease dynamics as well as divergent relationships between climate and coccidioidomycosis incidence. Future work should investigate the seasonal patterns and climate determinants of disease incidence in *C. posadasii*-dominant regions such as Arizona.

Conclusions
California's increasing drought risk, driven by global climate change, is expected to worsen with more frequent droughts and potential megadroughts.[50,51] Our findings, combined with recent research on drought's impact on coccidioidomycosis incidence, suggest that these changing climate patterns will affect both disease rates and seasonal patterns. Future droughts are likely to decrease annual incidence rates and suppress seasonal peaks during drought periods, resulting in lower but sustained cases year-round. Conversely, incidence rates and seasonality are expected to rise after droughts, leading to concentrated cases during specific months. The compounding effect of drought followed by heavy rainfall, a pattern projected to increase,[52] along with the geographic expansion of coccidioidomycosis, will continuously elevate disease risk for Californians. Further research is essential to understand the mechanistic connections between extreme climate events and coccidioidomycosis transmission to inform accurate disease prediction systems and mitigate future disease burden.

Data sharing statement
The coccidioidomycosis surveillance data used here is not publicly available and is only available with explicit permission from the California Department of Public Health.

Editor's note
The *Lancet* Group takes a neutral position with respect to territorial claims in published maps and institutional affiliations.

Disclaimer
The findings and conclusions in this article are those of the author(s) and do not necessarily represent the views or opinions of the California Department of Public Health or the California Health and Human Services Agency.

Declaration of interests
The authors declared no conflicts of interest.

Appendix A. Supplementary data
Supplementary data related to this article can be found at https://doi.org/10.1016/j.lana.2024.100864.

References
1 Obando-Pacheco P, Justicia-Grande AJ, Rivero-Calle I, et al. Respiratory syncytial virus seasonality: a global overview. *J Infect Dis.* 2018;217:1356–1364.
2 Tamerius J, Nelson MI, Zhou SZ, Viboud C, Miller MA, Alonso WJ. Global influenza seasonality: reconciling patterns across temperate and tropical regions. *Environ Health Perspect.* 2011;119:439–445.
3 Marr LC, Tang JW, Van Mullekom J, Lakdawala SS. Mechanistic insights into the effect of humidity on airborne influenza virus survival, transmission and incidence. *J R Soc Interface.* 2019;16:20180298.

4   Fisman DN. Seasonality of infectious diseases. *Annu Rev Public Health*. 2007;28:127–143.

5   Van Dyke MCC, Thompson GR, Galgiani JN, Barker BM. The rise of Coccidioides: forces against the dust devil unleashed. *Front Immunol*. 2019;10. https://doi.org/10.3389/fimmu.2019.02188.

6   Lewis ERG, Bowers JR, Barker BM. Dust devil: the life and times of the fungus that causes valley fever. *PLoS Pathog*. 2015;11. https://doi.org/10.1371/journal.ppat.1004762.

7   Centers for Disease Control and Prevention. *Valley fever statistics*. CDC; 2020. https://www.cdc.gov/fungal/diseases/coccidioidomycosis/statistics.html. Accessed October 27, 2020.

8   Cooksey GLS. Regional analysis of coccidioidomycosis incidence — California, 2000–2018. *MMWR Morb Mortal Wkly Rep*. 2020;69. https://doi.org/10.15585/mmwr.mm6948a4.

9   Gorris ME, Cat LA, Zender CS, Treseder KK, Randerson JT. Coccidioidomycosis dynamics in relation to climate in the southwestern United States. *GeoHealth*. 2018;2:6–24.

10 Martinez ME. The calendar of epidemics: seasonal cycles of infectious diseases. *PLoS Pathog*. 2018;14:e1007327.

11 Fisher FS, Bultman MW, Johnson SM, Pappagianis D, Zaborsky E. Coccidioides niches and habitat parameters in the southwestern United States: a matter of scale. *Ann N Y Acad Sci*. 2007;1111:47–72.

12 Sorenson RH. Survival characteristics of mycelia and spherules of coccidioides immitis in a simulated natural environment. *Am J Epidemiol*. 1964;80:275–285.

13 Egeberg RO, Elconin AE, Egeberg MC. Effect of salinity and temperature on coccidioides immitis and three antagonistic soil saprophytes. *J Bacteriol*. 1964;88:473–476.

14 Comrie Andrew C. Climate factors influencing coccidioidomycosis seasonality and outbreaks. *Environ Health Perspect*. 2005;113:688–692.

15 Head JR, Sondermeyer-Cooksey G, Heaney AK, et al. Effects of precipitation, heat, and drought on incidence and expansion of coccidioidomycosis in western USA: a longitudinal surveillance study. *Lancet Planet Health*. 2022;6:e793–e803.

16 Weaver EA, Kolivras KN. Investigating the relationship between climate and valley fever (coccidioidomycosis). *EcoHealth*. 2018;15:840–852.

17 Maddy KT. Ecological factors of the geographic distribution of Coccidioides immitis. *J Am Vet Med Assoc*. 1957;130:475–476.

18 Kolivras KN, Comrie AC. Modeling valley fever (coccidioidomycosis) incidence on the basis of climate conditions. *Int J Biometeorol*. 2003;47:87–101.

19 Tamerius JD, Comrie AC. Coccidioidomycosis incidence in Arizona predicted by seasonal precipitation. *PLoS One*. 2011;6. https://doi.org/10.1371/journal.pone.0021009.

20 Surveillance and Statistics Section, Infection Diseases Branch, Division of Communicable Disease Control, Center for Infectious Diseases. *Epidemiological summary of coccidioidomycosis in California, 2018*. California Department of Public Health; 2018. https://www.cdph.ca.gov/Programs/CID/DCDC/CDPH%20Document%20Library/CocciEpiSummary2018.pdf.

21 State of California, Department of Finances. *E-4 population estimates for cities, counties, and the state, 2001-2010, with 2000 & 2010 census counts*. Sacramento, CA. 2012.

22 State of California, Department of Finances. *E-4 population estimates for cities, counties, and the state, 2011-2020, with 2010 Census Benchmark*. Sacramento, CA. 2022.

23 Benedict K, Ireland M, Weinberg MP, et al. Enhanced surveillance for coccidioidomycosis, 14 US States, 2016. *Emerg Infect Dis*. 2018;24:1444–1452.

24 Tsang CA, Anderson SM, Imholte SB, et al. Enhanced surveillance of coccidioidomycosis, Arizona, USA, 2007–2008. *Emerg Infect Dis*. 2010;16:1738–1744.

25 Livneh B, Bohn TJ, Pierce DW, et al. A spatially comprehensive, hydrometeorological data set for Mexico, the U.S., and Southern Canada 1950–2013. *Sci Data*. 2015;2:150042.

26 National Center for Atmospheric Research Staff. *The climate data guide: PRISM high-resolution spatial climate data for the United States: max/min temp, dewpoint, precipitation*; 2017. https://climatedataguide.ucar.edu/climate-data/prism-high-resolution-spatial-climate-data-united-states-maxmin-temp-dewpoint.

27 Thornthwaite CW. An approach toward a rational classification of climate. *Geogr Rev*. 1948;38:55–94.

28 Vicente-Serrano SM, Beguería S, López-Moreno JI. A multiscalar drought index sensitive to global warming: the standardized precipitation evapotranspiration index. *J Clim*. 2010;23:1696–1718.

29 Svoboda M, LeComte D, Hayes M, et al. The drought monitor. *Bull Am Meteorol Soc*. 2002;83:1181–1190.

30 Roesch A, Schmidbauer H. *WaveletComp: Computational wavelet analysis*; 2018. https://CRAN.R-project.org/package=WaveletComp.

31 Gasparrini A, Armstrong B, Kenward MG. Distributed lag non-linear models. *Stat Med*. 2010;29:2224–2234.

32 Head JR, Sondermeyer-Cooksey G, Heaney AK, et al. Influence of meteorological factors and drought on coccidioidomycosis incidence in California, 2000–2020. *medRxiv*; 2022. 10.1101/2022.02.03.22270412.

33 United States Department of Agriculture. Natural resources conservation service. Web Soil Survey. https://websoilsurvey.nrcs.usda.gov/app/WebSoilSurvey.aspx. Accessed February 11, 2024.

34 Maddy KT. Observations on coccidioides immitis found growing naturally in soil. *Ariz Med*. 1965;22:281–288.

35 Schimel JP. Life in dry soils: effects of drought on soil microbial communities and processes. *Annu Rev Ecol Evol Syst*. 2018;49:409–432.

36 Evans SE, Wallenstein MD. Soil microbial community response to drying and rewetting stress: does historical precipitation regime matter? *Biogeochemistry*. 2012;109:101–116.

37 Egeberg RO, Ely AF. Coccidioides immitis in the soil of the southern san Joaquin Valley. *Am J Med Sci*. 1956;231:151–154.

38 Barker BM, Tabor JA, Shubitz LF, Perrill R, Orbach MJ. Detection and phylogenetic analysis of Coccidioides posadasii in Arizona soil samples. *Fungal Ecol*. 2012;5:163–176.

39 Kollath DR, Teixeira MM, Funke A, Miller KJ, Barker BM. Investigating the role of animal burrows on the ecology and distribution of Coccidioides spp. in Arizona soils. *Mycopathologia*. 2020;185:145–159.

40 Salazar-Hamm PS, Montoya KN, Montoya L, et al. Breathing can be dangerous: opportunistic fungal pathogens and the diverse community of the small mammal lung mycobiome. *Front Fungal Biol*. 2022;3. https://www.frontiersin.org/articles/10.3389/ffunb.2022.996574. Accessed January 6, 2023.

41 KeithT M, Crecelius HG. Establishment of Coccidiodies immitis in negative soil following burial of infected animal tissues. In: *The second symposium on coccidioidomycosis*. Tucson, Arizona: University of Arizona Press; 1965:309–312.

42 Prugh LR, Deguines N, Grinath JB, et al. Ecological winners and losers of extreme drought in California. *Nat Clim Change*. 2018;8:819–824.

43 Reheis MC. A 16-year record of eolian dust in Southern Nevada and California, USA: controls on dust generation and accumulation. *J Arid Environ*. 2006;67:487–520.

44 Tegen I, Werner M, Harrison SP, Kohfeld KE. Relative importance of climate and land use in determining present and future global soil dust emission. *Geophys Res Lett*. 2004;31. https://doi.org/10.1029/2003GL019216.

45 Okin GS, Reheis MC. An ENSO predictor of dust emission in the southwestern United States. *Geophys Res Lett*. 2002;29:46-1-46–3.

46 Das R, McNary J, Fitzsimmons K, et al. Occupational coccidioidomycosis in California: outbreak investigation, respirator recommendations, and surveillance findings. *J Occup Environ Med*. 2012;54:564–571.

47 California Department of Public Health (CDPH). *Preventing work-related coccidioidomycosis (valley fever)*. Electron. Libr. Constr. Occup. Saf. Health; 2013. https://elcosh.org/document/3684/d001224/preventing+work-related+coccidioidomycosis+(valley+fever).html. Accessed January 6, 2023.

48 Valley fever prevention. https://www.cdph.ca.gov/Programs/CID/DCDC/Pages/ValleyFeverPrevention.aspx. Accessed May 10, 2023.

49 Mead HL, Hamm PS, Shaffer IN, et al. Differential thermotolerance adaptation between species of Coccidioides. *J Fungi*. 2020;6:366.

50 Pierce DW, Kalansky JF, Cayan DR. *Climate, drought, and sea level rise scenarios for California's fourth climate change assessment*. La jolla. California: Scripps Institution of Oceanography; 2018.

51 Cook BI, Ault TR, Smerdon JE. Unprecedented 21st century drought risk in the American southwest and central plains. *Sci Adv*. 2015;1:e1400082.

52 Gershunov A, Shulgina T, Clemesha RES, et al. Precipitation regime change in western North America: the role of atmospheric rivers. *Sci Rep*. 2019;9:9944.